Stability of frozen waves in the modified Cahn-Hilliard model

E. S. Benilov,[*] W. T. Lee,[†] and R. O. Sedakov[‡]

MACSI, Department of Mathematics, University of Limerick, Ireland
(Received 7 January 2013; published 18 March 2013)

We examine the existence and stability of frozen waves in diblock copolymers with local conservation of the order parameter, which are described by the modified Cahn-Hilliard model. It is shown that a range of stable waves exists and each can emerge from a "general" initial condition (not only the one with the lowest density of free energy). We discuss the implications of these results for the use of block copolymers in templating nanostructures.

I. INTRODUCTION

The Cahn-Hilliard equation [1] is often used to model microstructures arising from spinodal decomposition in, say, polymer mixtures. One of the simplest systems exhibiting this behavior would be a mixture of two polymers made from monomers, A and B, with distinct chemical properties, e.g., if A is hydrophilic whereas B is hydrophobic. In such cases, a monomer unit is attracted to units of the same type while being repelled by the other type, implying that the most energetically favorable state is the one in which A and B units are fully segregated. Such a tendency is indeed confirmed by numerical modeling of the Cahn-Hilliard equation [2] and is also in agreement with stability analysis of similar models [3].

One feature of the Cahn-Hilliard model is that the order parameter is conserved globally (reflecting the mass conservation law). The standard model, however, can be modified for microstructures where the order parameter is conserved *locally* [4]. The modified model applies, for example, if chains of the A and B monomers are parts of the same polymer molecule, known as a "block copolymer" [5], in which case they can never be separated by a distance larger than the size of a single molecule.

Systems with a locally conserved order parameter are of particular interest in nanotechnology. In particular, block copolymers are used to template nanopatterns at surfaces, on scales that are too small for traditional top-down photolithography [6]. Such patterns have to be "directed" using chemical prepatterning or topography, which is known as graphoepitaxy and can provide excellent pattern registry [7]. In its simplest form, conventional lithographic techniques are used to create trenches in a silicon wafer—then the trenches are filled with a block copolymer which orders into lamellae parallel to the sidewall on annealing [8]. Finally, a selected monomer is chemically etched away and the remaining polymer used as an etch mask to facilitate pattern transfer to the substrate, creating nanowires on a scale too fine to be manufactured by conventional techniques [9,10].

The lamellae used to template the nanowires correspond to *frozen waves* (i.e., periodic time-independent solutions) of

the one-dimensional version of the modified Cahn-Hilliard equation. It is particularly important whether these solutions are unique or if perhaps multiple stable solutions exist, as the latter would impede one's control over the manufacturing process.

The present paper answers the above question by examining the existence and stability of frozen waves in the modified Cahn-Hilliard equation. In Sec. II, we shall formulate the problem mathematically. In Sec. III, the *existence* of frozen-wave solutions will be discussed. In Sec. IV, we shall present the results of a *stability* analysis of frozen waves.

II. FORMULATION

Consider a one-dimensional diblock polymer, with the characteristic thickness l of the A/B interface and mobility M (the latter characterizes the diffusion of the order parameter ϕ). Using l and l^2/M to nondimensionalize the spatial coordinate x and time t, respectively, we can write the one-dimensional version of the modified Cahn-Hilliard equation (MCHE) in the form

$$\phi_t + (\phi - \phi^3 + \phi_{xx})_{xx} + \alpha\phi = 0, \qquad (1)$$

where α determines the ratio of the characteristic size of the region over which the order parameter is conserved to l.

As shown in Ref. [11], the MCHE admits frozen waves only if

$$0 \leqslant \alpha < \tfrac{1}{4},$$

whereas the wavelength (spatial period) λ must satisfy

$$\frac{2\pi}{\sqrt{\frac{1}{2}(1 + \sqrt{1 - 4\alpha})}} < \lambda < \frac{2\pi}{\sqrt{\frac{1}{2}(1 - \sqrt{1 - 4\alpha})}} \qquad (2)$$

(see Fig. 1). Reference [11] also computed examples of frozen waves and the energy density E as a function of a frozen wave's length λ, which turned out to have a minimum at a certain $\lambda = \lambda_0$. Given that the energy cannot grow and is, thus, a Lyapunov functional, a conclusion was drawn that λ_0 is stable.

However, the fact that λ_0 minimizes the energy of frozen waves means only that the corresponding wave is stable with respect to perturbations *of its length*, but not necessarily to *arbitrary* perturbations (for which the "general" second

---

[*]Eugene.Benilov@ul.ie
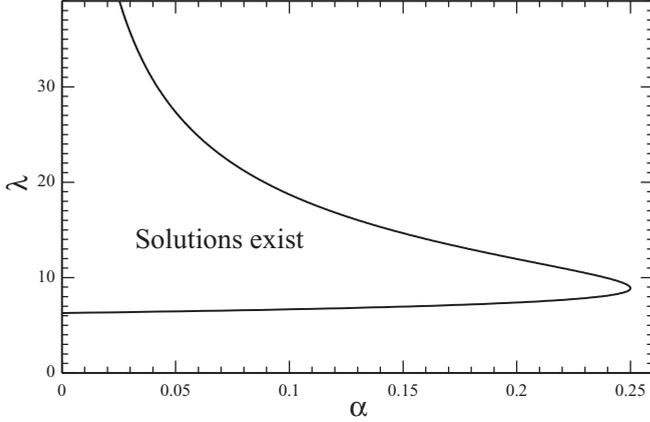[†]William.Lee@ul.ie
[‡]Roman.Sedakov@ul.ie

FIG. 1. The existence region of frozen waves (those described by one-wave solutions) on the (α,λ) plane [α is the parameter in the modified Cahn-Hilliard equation (1), λ is the wavelength]. The boundaries of the region are given by (2).

variation of E needs to be examined). On the other hand, stability rarely occurs for a single value of a parameter—hence, if λ_0 is indeed stable, it is likely to be one of a range of stable wavelengths.

In what follows, we shall clarify the above issues by examining the stability of frozen waves through the standard linear analysis, not involving energy arguments.

To do so, we introduce frozen waves as time-independent solutions, $\phi = \bar{\phi}(x)$, for which Eq. (1) yields

$$(\bar{\phi} - \bar{\phi}^3 + \bar{\phi}_{xx})_{xx} + \alpha\bar{\phi} = 0. \tag{3}$$

Together with the condition of spatial periodicity,

$$\bar{\phi}(x + \lambda) = \bar{\phi}(x), \tag{4}$$

Eq. (3) determines $\bar{\phi}(x)$.

To examine the stability of a frozen wave $\bar{\phi}(x)$, assume

$$\phi = \bar{\phi}(x) + \tilde{\phi}(t,x), \tag{5}$$

where $\tilde{\phi}$ describes a small disturbance. Substituting (5) into Eq. (1) and linearizing it, we obtain

$$\tilde{\phi}_t + (\bar{\phi} - 3\bar{\phi}^2\tilde{\phi} + \tilde{\phi}_{xx})_{xx} + \alpha\tilde{\phi} = 0. \tag{6}$$

We confine ourselves to disturbances with an exponential dependence on t (which are usually a reliable indicator of stability in general),

$$\tilde{\phi}(x,t) = \psi(x)e^{st}, \tag{7}$$

where s is the disturbance's growth (decay) rate. Substitution of (7) into (6) yields

$$s\psi + (\psi - 3\bar{\phi}^2\psi + \psi_{xx})_{xx} + \alpha\psi = 0. \tag{8}$$

Unlike the base wave $\bar{\phi}$, the disturbance ψ does not have to be periodic; it is sufficient that the latter is bounded at infinity. Given that ψ is determined by an ordinary differential equation with periodic coefficients [Eq. (8)], the assumption of boundedness amounts to the standard Floquet condition,

$$\psi(x + \lambda) = \psi(x)e^{i\theta}, \tag{9}$$

where θ is a real constant. Physically, condition (9) implies that, if the disturbance propagates by one wavelength of the base solution, the disturbance's amplitude remains the same, whereas its phase may change by a value of θ.

Equations (8) and (9) form an eigenvalue problem, where s and ψ are the eigenvalue and the eigenfunction. If, for some values of the phase shift θ, one or more eigenvalues exist such that $\mathrm{Re}\, s > 0$, the corresponding base wave $\bar{\phi}(x)$ is unstable.

III. FROZEN WAVE SOLUTIONS

It turns out that a lot of physically meaningful information about frozen waves can be obtained in the limit of weak nonlinearity, i.e., under the assumption

$$|\bar{\phi}| \ll 1.$$

To understand qualitatively what to expect in this case, one can simply omit the nonlinear term in Eq. (2) and seek a solution of the resulting linear equation in the form

$$\bar{\phi} = \varepsilon\cos(kx + p), \tag{10}$$

where the wave's amplitude ε and phase p are arbitrary, whereas the wave number k satisfies

$$-k^2(1 - k^2) + \alpha = 0. \tag{11}$$

Assuming $k > 0$ and recalling the relationship between the wavelength and the wave vector,

$$\lambda = \frac{2\pi}{k}, \tag{12}$$

one can see that, in the linear approximation, only two wavelengths are allowed—coincidentally, the same values which represent the upper and lower boundaries of the existence region (2), shown in Fig. 1. Under the *weakly nonlinear* approximation, in turn, one should expect the wavelength to be close, but not necessarily equal, to one of the above two values, with a deviation from them proportional to some degree of the wave's amplitude ε. Solutions similar to (10) are the ones computed in Ref. [11]; they will be referred to as "one-wave solutions."

To understand the physical meaning of *two*-wave solutions, seek a solution of the linearized version of Eq. (3) in the form

$$\bar{\phi} = \varepsilon_1\cos(k_1 x + p_1) + \varepsilon_2\cos(k_2 x + p_2), \tag{13}$$

where $\varepsilon_{1,2}$ and $p_{1,2}$ are arbitrary and $k_{1,2}$ are the roots of Eq. (11) such that

$$0 < k_1 < k_2. \tag{14}$$

Physically, solution (13) represents a superposition of two periodic waves of zero frequency, with wave numbers $k_{1,2}$ and phases $p_{1,2}$. Note that (13) is periodic only if k_2/k_1 (and, hence, λ_2/λ_1) are both rational numbers, which occurs only for some values of α (several examples of such are illustrated in Fig. 2).

The above linear analysis, however, leaves several important questions unanswered. On the (λ,α) plane, for example, one-wave solutions seem to exist near curve (11) and (12), whereas Ref. [11] found frozen waves only *inside* this curve,
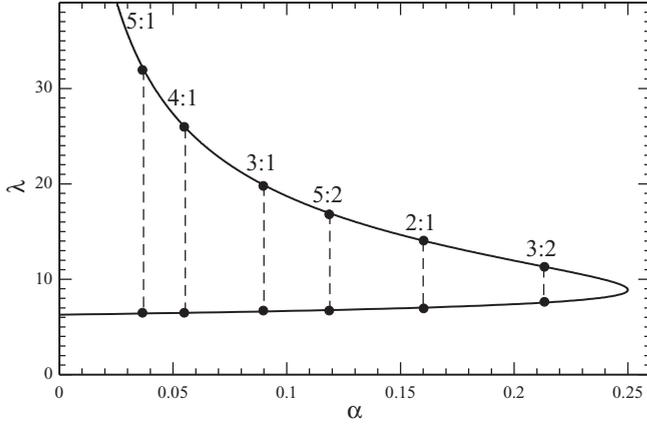
FIG. 2. A schematic illustrating linear two-wave solutions. The solid curve [determined by (11) and (12)] corresponds to linear frozen waves. The lengths $\lambda_{1,2}$ of the two "composite" waves are shown by dots and are connected by dashed lines. Two-wave solutions exist only for those values of α for which λ_2/λ_1 is a rational number (presented in the figure above the corresponding λ_2). The wavelength of a two-wave solution as a whole equals the lowest common multiple of λ_1 and λ_2.

and not *outside* (see Fig. 1). This discrepancy—as well as the question of the existence of two-wave solutions—will be clarified in Secs. III A and III B. The case of strong nonlinearity will be examined numerically for both types of frozen waves in Sec. III C.

A. Asymptotic results: One-wave solutions

It is convenient to change the spatial coordinate x to

$$\xi = kx$$

[where k is, again, the wave number determined by (12)]. In terms of ξ, Eqs. (3) and (4) become

$$k^2(\bar{\phi} - \bar{\phi}^3 + k^2\bar{\phi}_{\xi\xi})_{\xi\xi} + \alpha\bar{\phi} = 0, \tag{15}$$

$$\bar{\phi}(x + 2\pi) = \bar{\phi}(x). \tag{16}$$

We shall seek a solution as a series of the form

$$\bar{\phi} = \varepsilon(\bar{\phi}^{(0)} + \varepsilon^2\bar{\phi}^{(2)} + \cdots), \tag{17}$$

and also expand the wave number k,

$$k^2 = K^{(0)} + \varepsilon^2 K^{(2)} + \cdots. \tag{18}$$

To leading order, Eqs. (15) and (16) reduce to

$$K^{(0)}\big(\bar{\phi}^{(0)} + K^{(0)}\bar{\phi}^{(0)}_{\xi\xi}\big)_{\xi\xi} + \alpha\bar{\phi}^{(0)} = 0,$$
$$\bar{\phi}^{(0)}(x + 2\pi) = \bar{\phi}^{(0)}(x). \tag{19}$$

We seek a solution in the form

$$\bar{\phi}^{(0)} = A\cos(n\xi + p),$$

where A and p are real constants and $n > 0$ is an integer. It is sufficient to examine the case $n = 1$, as $n \geqslant 2$ corresponds to redefining the solution's spatial period by including more than one wavelength in it, without changing anything physically. We

also let $A = 1$ (as the wave's physical amplitude still remains arbitrary due to the arbitrariness of ε) and $p = 0$ (as a phase constant can always be included later). Thus, the leading-order solution becomes

$$\bar{\phi}^{(0)} = \cos\xi. \tag{20}$$

Substitution of (20) into (19) yields

$$K^{(0)} = \tfrac{1}{2}(1 \pm \sqrt{1 - 4\alpha}). \tag{21}$$

In the next-to-leading order, Eq. (15) yields

$$K^{(2)}\big(\bar{\phi}^{(0)} + K^{(0)}\bar{\phi}^{(0)}_{\xi\xi}\big)_{\xi\xi}$$
$$+ K^{(0)}\big(\bar{\phi}^{(2)} - \bar{\phi}^{(0)3} + K^{(2)}\bar{\phi}^{(0)}_{\xi\xi} + K^{(0)}\bar{\phi}^{(2)}_{\xi\xi}\big)_{\xi\xi} + \alpha\bar{\phi}^{(2)} = 0, \tag{22}$$

which, upon substitution of (20), becomes

$$K^{(0)}\big(\bar{\phi}^{(2)} + K^{(0)}\bar{\phi}^{(2)}_{\xi\xi}\big)_{\xi\xi} + \alpha\bar{\phi}^{(2)}$$
$$= \left(K^{(2)} - 2K^{(2)}K^{(0)} - \frac{3K^{(0)}}{4}\right)\cos\xi - \frac{9K^{(0)}}{4}\cos 3x. \tag{23}$$

This equation can have a 2π-periodic solution only if the term involving $\cos\xi$ on the right-hand side vanishes, which implies

$$K^{(2)} = \frac{3K^{(0)}}{4(1 - 2K^{(0)})}, \tag{24}$$

after which (24) yields

$$\bar{\phi}^{(2)} = \frac{9K^{(0)}}{36K^{(0)}(1 - 9K^{(0)}) - 4\alpha}\cos 3\xi. \tag{25}$$

Recalling that K is related to the wave number k by (18), and k is, in turn, related to the wavelength λ by (12), one can use expressions (21) and (24) to obtain

$$\lambda_{1,2} = \frac{2\sqrt{2}\pi}{\sqrt{1 \pm \sqrt{1 - 4\alpha}}}\left(1 \pm \frac{3\varepsilon^2}{8\sqrt{1 - 4\alpha}}\right) + O(\varepsilon^4), \tag{26}$$

where subscripts 1 and 2 correspond to $+$ and $-$, respectively. For $\varepsilon = 0$ (i.e., in the linear limit), λ_1 and λ_2 are the lower and upper boundaries of the existence interval in Fig. 1, whereas an increase in ε causes an increase in λ_1 and a decrease in λ_2. This means that one-wave solutions do not exist above $(\lambda_2)_{\varepsilon=0}$ and below $(\lambda_1)_{\varepsilon=0}$, which agrees with the conclusions of Ref. [11].

Observe that expansion (26) fails in the limit $\alpha \to \frac{1}{4}$. This case should be examined separately by assuming

$$\alpha = \tfrac{1}{4} + \varepsilon^2\alpha^{(2)}. \tag{27}$$

An expansion similar to the one above yields (technical details omitted)

$$k^2 = \tfrac{1}{2} \pm \sqrt{-\varepsilon^2\alpha^{(2)} - \tfrac{3}{8}\varepsilon^2} + O(\varepsilon^2), \tag{28}$$

from which λ can be readily found. The corresponding expansion of the solution is (technical details omitted)

$$\bar{\phi} = \varepsilon\big[\cos\xi - \tfrac{9}{128}\varepsilon^2\cos 3\xi + O(\varepsilon^4)\big]. \tag{29}$$

Formulas (28) and (29) describe the one-wave solution near the "tip" ($\alpha \to \frac{1}{4}$, $\lambda \to 2\sqrt{2}\pi$) of the existence region shown in Fig. 1. Formula (26), in turn, describes the solution near the boundary of the region, but not too close to its tip.

Finally, note that substitution of expression (21) for $K^{(0)}$ into expression (25) shows that $\bar{\phi}^{(2)}$ becomes infinite for

$$\alpha = \tfrac{9}{100}, \quad \lambda = 2\sqrt{10}\pi.$$

This is another example in which the straightforward expansion for the one-wave solution is inapplicable (in addition to the "tip point," $\alpha = \tfrac{1}{4}$, $\lambda = 2\sqrt{2}\pi$). The unbounded growth of the first-order term involving $\cos 3\xi$ suggests that, in this case, $\bar{\phi}^{(0)}$ should include both $\cos \xi$ and $\cos 3\xi$, and not just the former term, as solution (20) does.

This case will be examined in the next section.

B. Asymptotic results: Two-wave solutions

As mentioned above, two-wave solutions exist near those values of α for which the ratio of the wave numbers of the two individual waves is a rational number. Let $\alpha^{(0)}$ be one of such values, with $\alpha^{(2)}$ being a small deviation from it,

$$\alpha = \alpha^{(0)} + \varepsilon^2 \alpha^{(2)}. \tag{30}$$

Substitution of this expression, together with expansions (17) and (18), in Eq. (15) yields, to leading order,

$$K^{(0)}\big(\bar{\phi}^{(0)} + K^{(0)}\bar{\phi}^{(0)}_{\xi\xi}\big)_{\xi\xi} + \alpha^{(0)}\bar{\phi}^{(0)} = 0. \tag{31}$$

We assume that the two waves of which a two-wave solution consists have wave numbers $K^{(0)}n_1$ and $K^{(0)}n_2$, where $n_{1,2}$ are integers (without loss of generality, they can be assumed to be coprime and such that $n_1 > n_2 > 0$). Accordingly, we shall seek a solution of Eq. (31) in the form

$$\bar{\phi}^{(0)} = a \cos(n_1 x + \theta) + \cos n_2 x \tag{32}$$

(the fact that the second wave's amplitude is unity and its phase is zero does not reduce generality). Substituting (32) into (31), we obtain

$$\alpha^{(0)} = \frac{n_1^2 n_2^2}{\left(n_1^2 + n_2^2\right)^2}, \quad K^{(0)} = \frac{1}{n_1^2 + n_2^2}. \tag{33}$$

Recalling that K is related to the wavelength λ, one can see that these equalities determine the points in the (α, λ) plane near which two-wave weakly nonlinear solutions are localized (they are illustrated in Fig. 2).

To the next-to-leading order, (15) yields

$$K^{(0)}\big(\bar{\phi}^{(2)} + K^{(0)}\bar{\phi}^{(2)}_{\xi\xi}\big)_{\xi\xi} + \alpha^{(0)}\bar{\phi}^{(2)} = K^{(0)}\bigg(\frac{3a}{2}\cos(n_1 x + \theta) + \frac{a^3}{4}\left[3\cos(n_1 x + \theta) + \cos 3(n_1 x + \theta)\right]$$

$$+ \frac{3a^2}{4}\left\{\cos\left[(2n_1 - n_2)x + 2\theta\right] + \cos\left[(2n_1 + n_2)x + 2\theta\right]\right\} + \frac{3a}{4}\left\{\cos[(n_1 - 2n_2)x + \theta]\right.$$

$$+ \cos[(n_1 + 2n_2)x + \theta]\left.\right\} + \frac{3a^2}{2}\cos n_2 x + \frac{1}{4}\left(3\cos n_2 x + \cos 3n_2 x\right)\bigg)_{\xi\xi}$$

$$- a\left[K^{(2)}n_1^2\big(2K^{(0)}n_1^2 - 1\big) + \alpha^{(2)}\right]\cos(n_1 x + \theta) - \left[K^{(2)}n_2^2\big(2K^{(0)}n_2^2 - 1\big) + \alpha^{(2)}\right]\cos n_2 x.$$

This equation has a periodic solution for $\bar{\phi}^{(2)}$ only if the terms involving $\cos(n_1 x + \theta)$ and $\cos n_2 x$ cancel out, but the specifics depend on whether $(n_1, n_2) = (3, 1)$ or not.

In the former case, straightforward calculations yield

$$K^{(2)} = -\frac{3(7a^3 - a^2 + 17a + 3)}{340a}, \quad \alpha^{(2)} = -\frac{9(9a^3 + 3a^2 + 9a + 1)}{420a} \quad \text{if} \quad (n_1, n_2) = (3, 1),$$

whereas the latter case yields

$$K^{(2)} = -\frac{3\left[\left(n_1^2 - 2n_2^2\right)a^2 + 2n_1^2 - n_2^2\right]}{4\left(n_1^2 + n_2^2\right)\left(n_1^2 - n_2^2\right)}, \quad \alpha^{(2)} = -\frac{9n_1^2 n_2^2\left(a^2 + 1\right)}{4\left(n_1^2 + n_2^2\right)^2} \quad \text{if} \quad n_1 \neq 3n_2.$$

Now, using expressions (17), (18), (30), (12), (32), and (33) to relate $\bar{\phi}^{(2)}$, $K^{(2)}$, and $\alpha^{(2)}$ to the "physical" quantities, we can summarize the two-wave solution in the form

$$\bar{\phi} = \varepsilon\left[a\cos(n_1 x + \theta) + \cos n_2 x\right] + O(\varepsilon^3) \tag{34}$$

and

$$\alpha = \frac{9}{100} - \varepsilon^2 \frac{9(9a^3 + 3a^2 + 9a + 1)}{420a} + O(\varepsilon^4),$$

$$\lambda = 2\sqrt{10}\pi + \varepsilon^2 \frac{3\pi\sqrt{10}(7a^3 - a^2 + 17a + 3)}{34a} + O(\varepsilon^4),$$

$$\text{if} \quad (n_1, n_2) = (3, 1), \tag{35}$$

or

$$\alpha = \frac{n_1^2 n_2^2}{\left(n_1^2 + n_2^2\right)^2} - \varepsilon^2 \frac{9 n_1^2 n_2^2 \left(a^2 + 1\right)}{4 \left(n_1^2 + n_2^2\right)^2} + O(\varepsilon^4),$$

$$\text{if} \quad n_1 \neq 3 n_2. \quad (36)$$

$$\lambda = 2\pi \sqrt{n_1^2 + n_2^2} + \varepsilon^2 \frac{3\pi \left[\left(n_1^2 - 2 n_2^2\right) a^2 + 2 n_1^2 - n_2^2\right] \sqrt{n_1^2 + n_2^2}}{4 \left(n_1^2 - n_2^2\right)} + O(\varepsilon^4),$$

Expressions (35) and (36) can be viewed as parametric representations (with ε and a being the parameters) of the existence region of two-wave solutions with $n_{1,2}$, on the (α, λ) plane. It can be shown that, for all $n_{1,2}$, this region is a "semi-infinite sector" (see an example in Fig. 3). However, since we assumed weak nonlinearity, this conclusion can only be trusted near the vertices of the sectors. Effectively, we have found the tangent lines to the boundaries of the "true" region of the existence interval.

Observe that ε^2 can be eliminated from (35) and (36), which yields

$$\frac{\alpha - \frac{9}{100}}{\lambda - 2\sqrt{10}\pi} = -\frac{6(9 a^3 + 3 a^2 + 9 a + 1)}{27\sqrt{10}\pi(7 a^3 - a^2 + 17 a + 3)} + O(\varepsilon^2) \quad \text{if} \quad (n_1, n_2) = (3, 1), \quad (37)$$

or

$$\frac{\alpha - \frac{n_1^2 n_2^2}{\left(n_1^2 + n_2^2\right)^2}}{\lambda - 2\pi\sqrt{n_1^2 + n_2^2}} = -\frac{9 n_1^2 n_2^2 (a^2 + 1) \left(n_1^2 - n_2^2\right)}{3\pi \left(n_1^2 + n_2^2\right)^{5/2} \left[\left(n_1^2 - 2 n_2^2\right) a^2 + 2 n_1^2 - n_2^2\right]} + O(\varepsilon^2) \quad \text{if} \quad n_1 \neq 3 n_2. \quad (38)$$

For given $n_{1,2}$ and (α, λ), (37) and (38) can be treated as equations for a [it is, essentially, the ratio of the amplitudes of the waves which constitute the two-wave solution; see (34)]. Observe that (38) admits two roots for a (with equal magnitudes and opposite signs), which means that two-wave solutions with $n_1 \neq 3 n_2$ exist in pairs. In some cases these solutions can be obtained from each other by shifting $x \rightarrow x + \text{const}$ (for the 2:1 case, for example, $\text{const} = \pi$), but in other cases the solutions with positive and negative a seem to be genuinely different.

For the case $(n_1, n_2) = (3, 1)$, in turn, it follows from (38) that three roots exist for a. One of the three, however, corresponds to the *one*-wave solution. Indeed, recall that the expansion derived for those failed near $\alpha = \frac{9}{100}, \lambda = 2\sqrt{10}\pi$, i.e., precisely where the asymptotic theory for *two*-wave

FIG. 3. Regions of existence (bounded by the dotted line) of two-wave solutions with $\lambda_2/\lambda_1 = 2{:}1$. Thin solid lines show the boundaries of the existence region calculated under the assumption of weak nonlinearity. The thick solid line shows the existence region for one-wave solutions (as in Fig. 1).

solutions predicts the existence of those with $(n_1, n_2) = (3, 1)$. In fact, one- and two-wave solutions cannot be distinguished in this region, as, in both cases, the coefficients of $\cos 3x$ and $\cos x$ are of the same order.

C. Numerical results

In this section, we shall present examples of strongly nonlinear one- and two-wave solutions and the existence region for the latter. Two numerical methods have been used: the shooting method (which turned out to be insufficient for large wavelengths) and the method of Newton relaxation (which worked marginally better).

Figures 4(a) and 4(b) show examples of increasingly nonlinear one- and two-wave solutions, respectively, for a fixed wavelength λ and decreasing α. In Fig. 4(a), observe the increase of the wave's amplitude as α is moving away from the boundary of the existence region (for this value of λ, the boundary is located at $\alpha \approx 0.131$). Figure 4(b), in turn, illustrates the fact that the margins of the existence region for two-wave solutions correspond to the cases in which the amplitude of one of the two waves vanishes (which is how they bifurcate from one-wave solutions).

IV. THE STABILITY OF FROZEN WAVES

A. Asymptotic results

We shall first examine the stability of frozen waves asymptotically, under the same assumption of weak nonlinearity used to find the frozen waves themselves. We shall start by rewriting the stability problem (8) and (9) in terms of $\xi = kx$, which yields

$$s\psi + k^2(\psi - 3\bar{\phi}^2\psi + k^2\psi_{\xi\xi})_{\xi\xi} + \alpha\psi = 0, \quad (39)$$
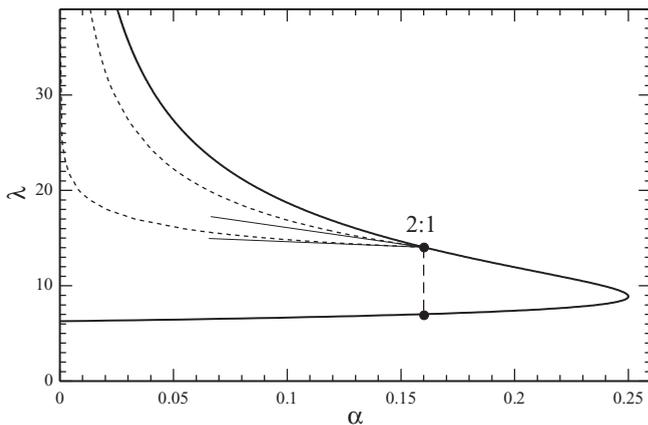
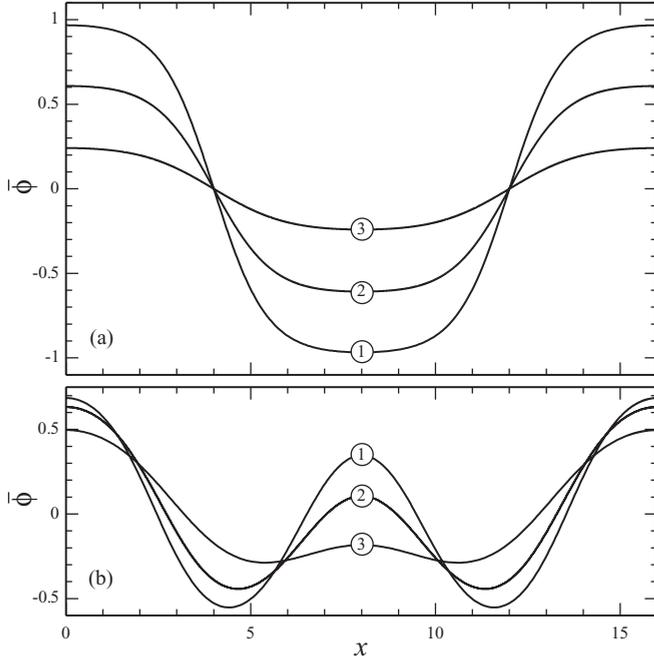$$\psi(\xi + 2\pi) = \psi(\xi)e^{i\theta}. \quad (40)$$

FIG. 4. Examples of frozen waves with spatial period $\lambda = 16$: (a) one-wave solutions with $\alpha = 0.005, 0.050, 0.100$ (curves 1, 2, and 3, respectively); (b) two-wave solutions with $\alpha = 0.07, 0.09, 0.11$ (curves 1, 2, and 3, respectively).

It turns out that all weakly nonlinear solutions, one- and two-wave alike, are unstable for all α except $\alpha \to \frac{1}{4}$ (i.e., except the "tip" of the existence interval for one-wave solutions shown in Fig. 1). We emphasize that this conclusion does not apply to *strongly* nonlinear waves (which can be either stable or unstable for any α; see the next section). Thus, assuming that $\alpha = \frac{1}{4} + O(\varepsilon^2)$, we represent α by expression (27); the corresponding base solution, $\bar{\phi}$, is represented by (28) and (29).

A straightforward analysis shows that, if the phase shift θ is order 1, all solutions of the eigenvalue problem (39) and (40), with the parameters determined by (27)–(29), are stable. Thus, instability can occur only for small θ, which can be conveniently accounted for by letting

$$\theta = 2\pi \varepsilon q, \tag{41}$$

where q is an order-1 constant. Note that the smallness of the phase shift θ implies that the instability occurs at wavelengths close to that of the base solution.

It is also convenient to introduce

$$\psi_{\text{new}} = \psi e^{-i\varepsilon q x}. \tag{42}$$

Using (41) and (42) to replace θ and ψ in Eqs. (39) and (40) with q and ψ_{new}, we obtain (subscript "new" omitted)

$$s\psi + k^2(\psi + k^2\psi_{\xi\xi} - 3\varepsilon^2\phi^2\psi)_{\xi\xi} + i\varepsilon q k^2(2\psi_\xi + 4k^2\psi_{\xi\xi\xi}) \\ - \varepsilon^2 q^2 k^2(\psi + 6k^2\psi_{\xi\xi})_{\xi\xi} + O(\varepsilon^3) + \alpha\psi = 0, \tag{43}$$

$$\psi(\xi + 2\pi) = \psi(\xi), \tag{44}$$

where the specific form of the terms $O(\varepsilon^3)$ will not be needed.

It can be demonstrated that no instability occurs if $s = O(1)$, hence only small s needs to be examined. We assume

(and shall eventually justify by obtaining a consistent asymptotic expansion) that

$$s = \varepsilon^2 s^{(2)} + \cdots,$$

while the eigenfunction is

$$\psi = \psi^{(0)} + \varepsilon^2 \psi^{(2)} + \cdots.$$

To leading order, Eqs. (43), (44), and (27)–(29) reduce to

$$\frac{1}{2}\left(\psi^{(0)} + \frac{1}{2}\psi^{(0)}_{\xi\xi}\right)_{\xi\xi} + \frac{1}{4}\psi^{(0)} = 0,$$

$$\psi^{(0)}(\xi + 2\pi) = \psi^{(0)}(\xi),$$

which yield

$$\psi^{(0)} = S \sin x + C \cos x, \tag{45}$$

where S and C are undetermined constants.

In the next-to-leading order, Eqs. (43), (44), and (27)–(29) yield (after straightforward algebra)

$$\frac{1}{2}\left(\psi^{(2)}_{\xi\xi} + \frac{1}{2}\psi^{(2)}_{\xi\xi\xi\xi}\right) + \frac{1}{4}\psi^{(2)} + \frac{3}{4}\Big[S \sin x + C \cos x \\ + \frac{1}{2}S(3\sin 3x - \sin x) + \frac{1}{2}C(3\cos 3x + \cos x)\Big] \\ + \left(s^{(2)} + q^2 - \frac{3}{8}\right)(S \sin x + C \cos x) \\ - 2iq\sqrt{-\alpha^{(2)} - \frac{3}{8}}\,(S \cos x - C \sin x) = 0,$$

$$\psi^{(2)}(\xi + 2\pi) = \psi^{(2)}(\xi).$$

This boundary-value problem has a solution for $\psi^{(2)}$ only if

$$\frac{3}{8}S + \left(s^{(2)} + q^2 - \frac{3}{8}\right)S + 2iq\sqrt{-\alpha^{(2)} - \frac{3}{8}}\,C = 0,$$

$$\frac{9}{8}C + \left(s^{(2)} + q^2 - \frac{3}{8}\right)C - 2iq\sqrt{-\alpha^{(2)} - \frac{3}{8}}\,S = 0,$$

which, in turn, has a solution for S and C only if

$$s^{(2)2} + \left(2q^2 + \frac{3}{4}\right)s^{(2)} + q^2\left[q^2 + \frac{3}{4} - 4\left(-\alpha^{(2)} - \frac{3}{8}\right)\right] = 0.$$

This equation determines the eigenvalue $s^{(2)}$. It can be readily shown that $s^{(2)}$ is stable (i.e., Re $s^{(2)} < 0$) for all q only if

$$\alpha^{(2)} < -\frac{9}{16}.$$

Finally, using (27) and (28) to express $\alpha^{(2)}$ in terms of the "physical" parameters α and λ, we obtain the following stability criterion for a frozen wave with parameters (α, λ):

$$(\lambda - 2\sqrt{2}\pi)^2 \lesssim \frac{8}{3}\pi^2\left(\frac{1}{4} - \alpha\right). \tag{46}$$

Observe that, for any $\alpha < \frac{1}{4}$, there exists an *interval* of stable wavelengths, not just a single value of λ.

As mentioned before, condition (46) applies only if α is close to $\frac{1}{4}$. In the next subsection, it will be extended numerically to arbitrary values of α.

B. Numerical results

The eigenvalue problem (8) and (9) was solved numerically for $\psi(x)$ and s with the base wave $\bar{\phi}(x)$ computed using problem (3) and (4). The general features of the dispersion relation [the dependence $s(\theta)$] of the eigenvalue problem (8) and (9) are described in the Appendix, whereas here we shall only present the stability diagram on the (α, λ) plane; see Fig. 5. Evidently, for all values of α, an interval of λ exists where one-wave solution are stable, which confirms and extends the
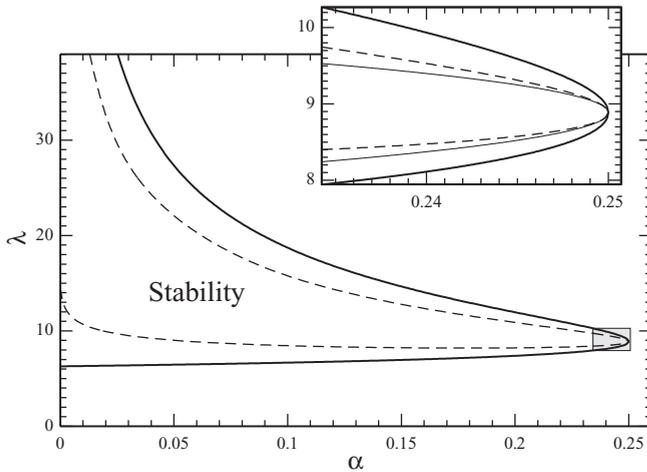
FIG. 5. The stability region of one-wave solutions on the (α,λ) plane (shown by the dashed line). The thick solid line shows the existence region of one-wave solutions (as in Fig. 1). The upper panel represents a blow-up of the shaded region of the lower panel [the thin solid line shows the stability region's asymptotic boundary, (46)].

asymptotic $(\alpha \to \frac{1}{4})$ stability criterion (46). We have not found any stable two-wave solutions, which suggests they are either unstable or perhaps their regions of stability are small and difficult to locate.

To illustrate that *any* solution from the range of stable frozen waves (not necessarily the wave with the minimum free-energy density) can emerge from a "general" initial condition, we have carried out the following numerical experiment. The time-dependent MCHE (1) was simulated using finite differences with a fully implicit backwards Euler method, and the results of the simulations presented below are for $\alpha = 0.1$.

In this case, the energy minimizing wavelength is $\lambda_0 = 11.31$ (calculated from the interpolation formula of Ref. [11]), with the corresponding frozen-wave solution denoted by $\phi_0(x)$. According to our analysis, however, a solution $\phi_1(x)$ with the commensurate wavelength $\lambda_1 = 14.13$ ($\lambda_0/\lambda_1 = 4/5$) should also be stable.
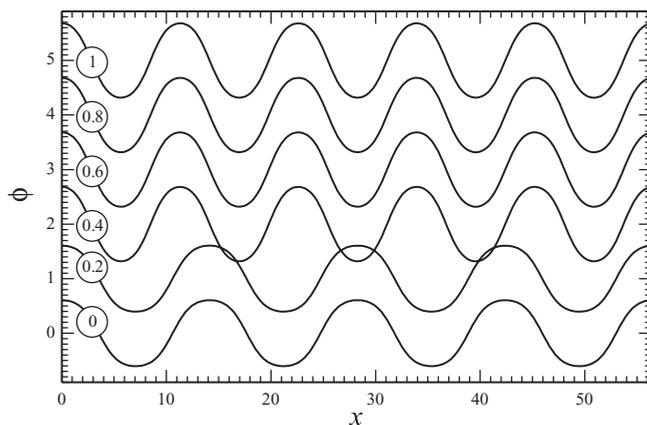

FIG. 6. Evolution of perturbed steady states within the stable region at $\alpha = 0.1$. The traces show the limiting $(t \to \infty)$ solution initialized by (47) for various β. The traces are incremented in steps of 0.5, beginning with zero increment for $\beta = 0$ (the lowest trace) and ending for $\beta = 1$ (the highest trace). The curves are marked with the corresponding values of β.

To verify this, Eq. (1) was simulated in a domain of size $L = 5\lambda_0 = 4\lambda_1$, which accommodates both solutions. The initial condition was chosen as a "mixture" of the frozen waves $\phi_0(x)$ and $\phi_1(x)$, i.e.,

$$\phi(x,0) = \beta\phi_0(x) + (1 - \beta)\phi_1(x), \qquad (47)$$

where $\beta \in (0,1)$ is the "mixing ratio." The time step was 0.1 and 400 grid points per period were used, and it has been verified that the results were mesh- and time-step-independent.

If $\phi_0(x)$ was the only stable solution, the system would evolve toward ϕ_0 for all β. Our simulations nevertheless show that, for $\beta = 0.2$, the system evolves back to ϕ_1 (see Fig. 6), which confirms our conclusion about the existence of *multiple* stable states.

V. CONCLUDING REMARKS

The main result of the present paper is illustrated in Fig. 5, which shows the stability region of (one-wave) frozen solutions of the modified Cahn-Hilliard equation (1). We have also found a previously unknown class of frozen waves—the "two-wave solutions"—but these seem to be unstable and, thus, less important than the usual, one-wave type.

We have also made a more general—and potentially more important—conclusion regarding the energy approach to studies of stability. If a family of solutions exists and one of them minimizes the energy functional, this does not necessarily mean that all other solutions are unstable. Furthermore, the stability of the minimizer solution cannot be guaranteed either: even though it is stable with respect to the perturbation of 'shifting along the family of solutions, another perturbation can still destabilize it.

Physically, our results imply that when lamellar microstructures of block copolymers are used to template nanowires, one must ensure that only the desired state is created. This may become more of a critical concern as larger numbers of nanowires are to be created within a single trench. In practice, some control over this can be exerted via the annealing schedule. It should also be noted that a kinetically stable quenched state may be selected rather than a true time-independent solution to the modified Cahn-Hilliard equation.

Finally, it would be interesting to extend the present results to steady states with *two* spatial dimensions, similar to those found in Ref. [12] for an equation similar to the two-dimensional MCHE (but with a slightly different nonlinearity).

APPENDIX: THE STRUCTURE OF THE DISPERSION RELATION AND THE EIGENFUNCTIONS OF THE EIGENVALUE PROBLEM (8) AND (9)

First of all, it can be readily shown (and has been confirmed numerically) that the eigenvalue s of problem (8) and (9) is real.
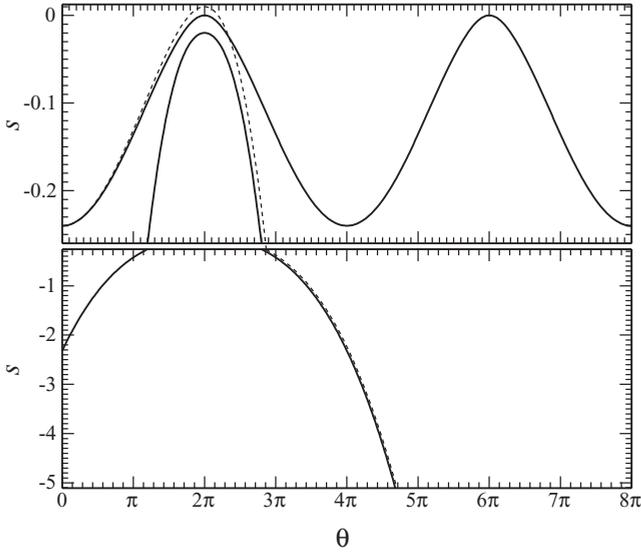
FIG. 7. The dispersion relation $s(\theta)$ for the eigenvalue problem (8) and (9) with $\alpha = 0.24$, $\lambda = 8.886$ (solid line). The dotted line shows the limiting dispersion curve (A2). Note the difference in the vertical axes' scales of the upper and lower panels.

Observe also that, for the boundary points of the existence region (see Fig. 1), frozen waves have zero amplitude, i.e., $\bar{\phi} = 0$. In this case, the eigenfunction of problem (8) and (9) can be readily found,

$$\psi = \exp\frac{i\theta x}{\lambda},\qquad (A1)$$

as well as the dispersion relation (i.e., the dependence of the eigenvalue s on the phase shift θ),

$$s = -\alpha + \left(\frac{\theta}{\lambda}\right)^2 - \left(\frac{\theta}{\lambda}\right)^4.\qquad (A2)$$

Observe that, as follows from (A1), the eigenfunction becomes more and more oscillatory with increasing θ.

In the general case (i.e., for *interior* points of the existence region of frozen waves, where $\bar{\phi} \neq 0$), one would expect that (A2) is somehow perturbed, but still keeps its structure as a single curve on the (θ, s) plane. Furthermore, the large-θ part of the "general" dispersion relation should not differ much from that of (A2) as, for rapidly oscillating ψ, the term involving $\bar{\phi}$ in Eq. (8) is negligible.

Our computations show, however, that, no matter how small $\bar{\phi}$ is, the dispersion relation splits into two branches; see Fig. 7.

The following properties of the two branches have been observed:

(i) The upper branch is periodic with a period of 4π.

(ii) Both branches are symmetric with respect to $\theta = 2\pi$ (provided they are extended to negative θ).

As a result, the only "original" part of the upper branch is the segment $\theta \in [0, 2\pi]$, whereas the "original" part of the lower branch is that for $\theta = [2\pi, \infty)$. Not surprisingly, the unperturbed dispersion relation (A2) "switches" from the upper branch to the lower one near the point $\theta = 2\pi$ (see Fig. 7).

Figure 8 shows typical behavior of the eigenfunctions: for $\theta = 0$, $\psi(x)$ does not oscillate at all; for $\theta = 2\pi$, it oscillates once; for $\theta = 4\pi$, it oscillates twice, etc.
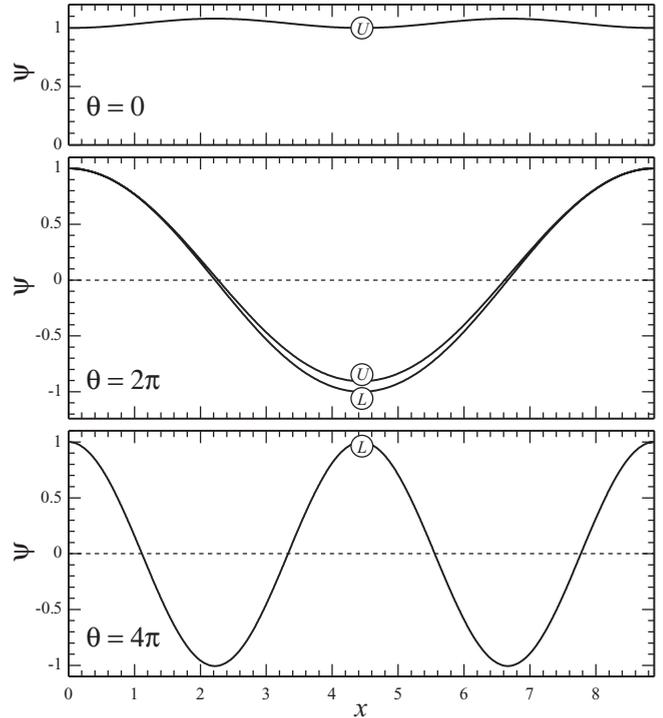

FIG. 8. Examples of eigenfunctions of problem (8) and (9) with $\alpha = 0.24$, $\lambda = 8.886$. The eigenfunctions marked with U and L correspond to the upper and lower branches, respectively, of the dispersion relation illustrated in Fig. 6.

Figure 9, in turn, shows the onset of instability brought by a change of the period of the base wave. One can see that the waves with $\theta \approx 2\pi$ are first to lose stability (which agrees with our asymptotic analysis of the case $\alpha \to \frac{1}{4}$).

Finally, we mention that two exact solutions were found for the eigenvalue problem (8) and (9):

$$s = -\alpha \qquad \text{for} \qquad \theta = 0,\qquad (A3)$$

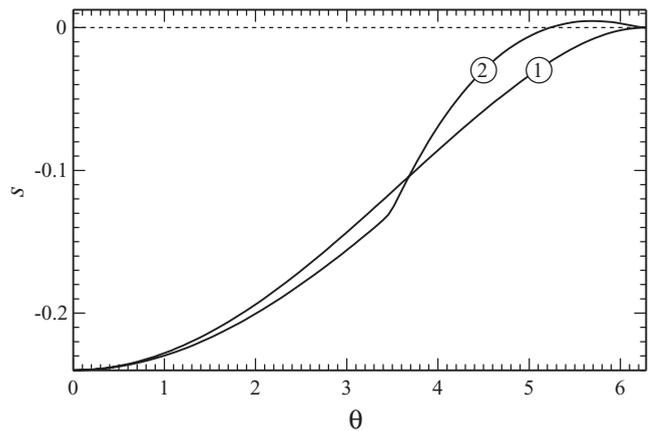$$s = 0 \qquad \text{for} \qquad \theta = 2\pi.\qquad (A4)$$

FIG. 9. The dispersion curves (upper branches) for $\alpha = 0.24$ and (1) $\lambda = 8.886$ (stability for all θ), (2) $\lambda = 9.786$ (instability for sufficiently small θ).

In the latter case, the disturbance can be found analytically, $\psi = \bar{\phi}$, and it corresponds to an infinitesimal shift of the base wave. The former solution does not seem to have an obvious physical meaning [nor does it admit an obvious analytical expression for the eigenfunction, as Eq. (A4) has been established numerically].

---

[1] W. G. Carter, J. E. Taylor, and J. W. Cahn, JOM-J. Miner. Met. Mater. Soc. **49**, 30 (1997).

[2] E. V. L. de Mello and O. T. S. Filho, Physica A **347**, 429 (2005).

[3] E. S. Benilov and M. Chugunova, Phys. Rev. E **81**, 036302 (2010).

[4] T. Ohta and K. Kawasaki, Macromolecules **19**, 2621 (1986).

[5] N. Hadjichristidis, S. Pispas, and G. Floudas, *Block Copolymers: Synthetic Strategies, Physical Properties, and Applications* (Wiley, New Jersey, 2003).

[6] T. G. Fitzgerald, R. A. Farrell, N. Petkov, C. T. Bolger, M. T. Shaw, J. P. F. Charpin, J. P. Gleeson, J. D. Holmes, and M. A. Morris, Langmuir **25**, 13551 (2009).

[7] K. O. Stuen, F. A. Detcheverry, G. S. W. Craig, C. S. Thomas, R. A. Farrell, M. A. Morris, J. J. de Pablo, and Paul F. Nealey, Nanotechnology **21**, 495301 (2010).

[8] R. A. Farrell, N. Petkov, M. A. Morris, and J. D. Holmes, J. Colloid Interface Sci. **349**, 449 (2010).

[9] D. Borah, M. T. Shaw, S. Rasappa, R. A. Farrell, C. O'Mahony, C. M. Faulkner, M. Bosea, P. Gleeson, J. D. Holmes, and M. A. Morris, J. Phys. D **44**, 174012 (2011).

[10] R. A. Farrell, N. T. Kinahan, S. Hansel, K. O. Stuen, N. Petkov, M. T. Shaw, L. E. West, V. Djara, R. J. Dunne, O. G. Varona, P. G. Gleeson, S. J. Jung, H. Y. Kim, M. M. Kolesnik, T. Lutz, C. P. Murray, J. D. Holmes, P. F. Nealey, G. S. Duesberg, V. Krstic, and M. A. Morris, Nanoscale **4**, 3228 (2012).

[11] F. Liu and N. Goldenfeld, Phys. Rev. A **39**, 4805 (1989).

[12] R. Choksi, M. Maras, and J. F. Williams, SIAM J. Appl. Dyn. Sys. **10**, 1344 (2011).